APPROVAL SHEET

Title of Thesis: Cooling Pad Effectiveness to Lower Temperature in Human Tissue: Theoretical Simulations and Experiments

Name of Candidate: Alexander Caporale

Master of Science, 2022

Thesis and Abstract approved:

Liang Zhu

Professor

Department of Mechanical Engineering

University of Maryland Baltimore County

Date Approved: April 25, 2022

Abstract

Title of Thesis: COOLING PAD EFFECTIVENESS TO LOWER TEMPERATURE IN HUMAN TISSUE: THEORETICAL SIMULATIONS AND EXPERIMETNS

Alexander Caporale, Masters of Science, 2022

Thesis direct by: Dr. Liang Zhu,

Professor

Department of Mechanical Engineering

University pf Maryland Baltimore County

A combined experimental and theoretical simulation approach was developed to evaluate performances of a surface cooling pad in reducing temperatures in human knee tissue. Experiments were performed on healthy volunteers to collect skin temperature values under a cooling pad during cooling sessions of 20 minutes. Then a whole-body heat transfer model was developed to extract the unknown overall heat transfer coefficient. Parametric studies were conducted to investigate the effects of the coolant temperature and overall heat transfer coefficient on the tissue temperature field. The simulation results demonstrated the effectiveness of the cooling pad in reducing temperatures by at least 2°C (37°C to 35°C) within a tissue region less than 34 mm under the cooling pad. This was achieved with a coolant temperature of 0°C for a cooling duration of 20 minutes. Results of this study would provide information to clinicians on whether to prescribe cooling therapy to patients after surgery.

Cooling Pad Effectiveness To Lower Temperature in Human Tissue: Theoretical Simulations and Experiments

By

Alexander Caporale

Thesis submitted to the Faculty of the Graduate School of the

University of Maryland, Baltimore County, in partial fulfillment

of the requirements for the degree of

Master of Science

2022

To My Grandpa Lou

Acknowledgements

First, I express my greatest appreciation to my advisor, Dr. Liang Zhu, for giving me tremendous help to work on this experimental and simulation project. Her guidance and support made this study possible.

I would like to thank Dr. Meilin Yu and Dr. Ronghui Ma, in addition to Dr. Zhu, for being members of my thesis committee, and for taking your time and patience to read my thesis. My gratitude extends to the faculty and staff of the Department of Mechanical Engineering at the University of Maryland Baltimore County for helping me in my studies while at UMBC. Additionally, I would like to thank Manpreet Singh and Jacob Lombardo for making my time at UMBC enjoyable and for volunteering to help me in this study.

I want to thank my grandmother, parents, and brothers for their continued love and support during this study.

Finally, I wish to express my loving thanks to Grandpa Lou, who passed away during my time at UMBC. I will miss him immensely, especially his unending love and support of me.

Table of Contents

List of Tables

Description **Page**

List of Figures

Description **Page**

Chapter 1: Introduction

1.1 Overview

This M.S. thesis research is aimed to evaluate the effectiveness of skin cooling pads on lowering the temperature in human tissue using both theoretical simulations and experimental measurements. The cooling penetration to deep tissue, if successful, would demonstrate an alternative method to relieve pain during post-surgery recovery, rather than using pain relief medications. When patients are advised to use cooling pads post-surgery, immediate pain reduction may not be evident. However, discomfort due to cold sensation and decrease in body core temperature often results in discontinuity of the cooling session, and those patients often turn toward opioids or other medications for their immediate relief of the pain [Cleveland Clinic Medical Professional 2020]. Since cooling must penetrate to the deep tissue of the surgical repair site, unknown cooling penetration depth and possible systemic hypothermia do not add confidence to both physicians and patients to advocate the widespread use of this method. In this thesis research, a combined experimental and theoretical simulation approach was designed to collect data and predict thermal performance of skin cooling pads on its potential use of reducing pain, inflammation, and swelling at surgical sites. To accomplish this, both theoretical simulations and experiments were implemented to determine thermal/physical parameters that allow predictions of cooling penetration to targeted tissue under various combinations of cooling parameters. Experiments were conducted on healthy volunteers to collect body temperature change and to map skin surface temperatures before and after applying a commercially available cooling pad on the leg surface of human volunteers. Theoretical simulations were then conducted on a generated whole-body heat transfer

model to extract physical/thermal parameters. Finally, parametric studies were conducted to evaluate the influence of various cooling parameters on the temperature field in the tissue.

1.2 Background

1.2.1 Data of Surgeries Performed in the U.S.

In the U.S., there are approximately 48.3 million surgeries performed annually [Hall et al., 2017]. The types of surgeries pertain to operations on the digestive system, the eye, the musculoskeletal system, the integumentary system, and the nervous system. Each surgery has its own subset of specific operations and has their own operating time duration [Hall et al., 2017]. Surgeries are typically performed either to remove tissue such as tumors, or to repair soft or hard tissues. After operations, patients experience discomforts and complications around the incision site, resulting in local soreness, pain, and swelling that are typical post-surgical consequences. Systemic complications may also occur, such as shock, bleeding, deep vein thrombosis (blood clot), pulmonary embolism (blood clot in lungs), lung problems, urinary retention (trouble with bladder), and a reaction to anesthesia [Sudheendra et al., 2021]. Duration of observation immediately after surgery is around 70 minutes, although it varies from surgery to surgery [Hall et al., 2017]. Then, the patient is sent home. Most patients need days or weeks to recover from the surgery and for the wound to heal [Miller et al., 2014]. Factors that affect the recovery duration after a surgery are determined by types of surgery the patient underwent, complications after the surgery, wound care, and methods of recovery the patient is prescribed [Miller et al., 2014].

1.2.2 Post-Surgery Recovery Methods

Recovery duration after surgery varies, and it is affected by what kind of surgery a patient underwent and the complications that may have resulted from the operation. Recovery methods are split into two aspects: physical and medication approaches. Physical approaches involve physical therapy, bed resting, or thermal treatments. The second approach is prescribing medications that are often pain-killers including prescription of opioids or over-the-counter medications such as ibuprofen and acetaminophen for reducing pain or fevers. The use of medications is straight forward and easy to implement. On the other hand, physical approaches require monitoring or help from medical personnel. For example, physical therapy of implementing exercises to increase blood supply to the affected region to promote healing, requires supervision of a licensed physical therapist. It is common to prescribe physical therapy to patients for improving movement in limbs after surgeries of joint replacement or tendon reconstruction. Thermal treatment after surgery often involves cooling or heating tissue. Commercially available cooling or heating systems are prescribed to patients to have the sessions at home, typically without staff supervision. In the past, thermal treatments can be prescribed in conjunction with physical therapy. It has already been implemented in sport medicine and in first-aid practices of applying cold compresses to sores or sprains.

1.2.3 Cold Therapy

Cold therapy is defined as a low temperature treatment method for diseased tissue or to decrease secondary biochemical reactions after the initial injury. When the temperature used in a cold therapy is way below 0°C, it is called cryotherapy, and its

main goal is to freeze or destroy abnormal tissue. A helpful review on this topic is given by Dr. Chato [Chato 1992]. In the 19th century, scientists generated coolants by rapid evaporation of a warm jet of air [Bouganim and Anatoli 2005; Chato 1992]. In the early 1900s, carbon dioxide snow was suggested as a coolant for cryotherapy. These earliest freezing methods were primarily used to treat skin disorders. Cryotherapy applications accelerated around the 1960s, initially being applied to the surface of brain tissue. Later, the development of freezing cannulas allowed localized treatment to tissue damage inside the central nervous system [Bouganim and Anatoli 2005; Chato 1992]. In the past decades, improvement of the cryotherapy probe has broadened the applications, and it is used to treat a variety of skin conditions, brain disorders such as cerebral palsy and Parkinson's disease, and various tumors [Bouganim and Anatoli 2005; Chato 1992]. Inputs from engineers allowed the use of calculations and simulation predictions for the size of the frozen region in the vicinity of the cryoprobe [Cleveland Clinic Medical Professional 2020]. Adjustment of cooling parameters was also available during a cooling session. Doctors have recommended the treatment to minimize invasive surgical procedures. In addition, previous studies have demonstrated that patients undergoing cryotherapy recovered quickly with little pain due to lowered nerve signals by cooling [Cleveland Clinic Medical Professional 2020].

A cooling system with a coolant temperature equal to or higher than 0°C falls into the second group of cold therapy, often seen in home use. Home-use cooling systems typically use water or water/ice mixture as the coolant for a cooling session of 15-60 minutes. The treatment session can be done in a more relaxed environment than going to the doctor's office.

Following any local tissue injury, it is recommended to place something cold on the injured site. It has been suggested that even a temperature decrease of 1 or 2°C in tissue decreases local inflammation after an injury. Local heating to the site is recommended to patients to implement later to deliver hormones and other necessary chemicals to the region to promote healing. Following an injury, inflammation always occurs. Inflammation is a process during which human body's white blood cells and their by-products protect the person from bacteria and virus infections [Zelman 2020]. Unfortunately, local inflammation acts like a double-edged sword. On one side, it is essential for triggering the immune system's response. When an inflammation occurs in a body, different immune system cells may be involved. They release various substances, known as inflammatory hormones, such as bradykinin and histamine. This causes the small blood vessels in the tissue to dilate, allowing more blood to reach the injured tissue. For this reason, inflamed areas turn red and feels hot. The increased blood flow also allows more immune system cells to be carried to the injured tissue, where they help with the healing process. Unfortunately, inflammation causes pain due to those hormones irritating more local nerves. As a result, it sends more pain signals to the brain. For most patients, the resulting pain is often unbearable, and it prevents them from resuming normal life.

The biochemical mechanisms involved in cold therapy above freezing temperature are complicated. Initially, researchers believed that above-freezing cooling may decrease the blood perfusion rate at the injured site, like cold-induced halting of bleeding. For example, oxygen consumption in tissue can decrease by 5% – 7% for each degree Celsius reductions in tissue temperature [Abramson et al., 1958; Diao et al., 2003;

Hoffman et al., 1982; Smith and Zhu 2010]. Since local metabolism is coupled with local blood perfusion rate, cooling also decreases local metabolic rate following a similar extent. Later, clinicians found that cooling played a key role in minimizing deleterious biochemical reactions in the secondary injury triggered by the initial trauma [Carney et al., 2016; Maier et al., 2002; Marion et. al., 1996; Yenari et al., 2000]. The secondary injury is often more fatal than the initial trauma to patients. Reports of celebrators dying from secondary injuries were occasionally heard of in the past, possibly due to their failure to seek medical treatment following the initial head injury. It has been demonstrated that even a very mild cooling of several degrees Celsius would delay occurrence or minimize the extent of the secondary injury. Specifically, cooling modifies a wide range of cell necrosis mechanisms as well as slowing down propagation of cascade and pathological excitation in biochemical reactions. Thus, implementation of cooling leads to inhibiting inflammation in the first place, reducing pain, limiting edema formation, and promoting tissue healing [Pierce-Smith et al., 2020; Smith and Zhu 2010; Xu et al., 2002].

On another front, even if there is no local infection after a surgery, the cutting of the skin alone during a surgery always stimulates nerve fibers to send pain signals to the brain. As the body begins to heal, pain should decrease and eventually stop. During the healing process, localized cooling can be used to decrease nerve activity via slowing down sodium permeability of axons, therefore, resulting in slow neural conduction to block pain signals traveling along nerves [Augustine 2004; Dhavalikar et al., 2009].

1.2.4 Cooling Systems

Typical commercial cooling systems are easy to be purchased online. Those systems are the same with a few variations, shown in Figure 1.1. Each system has a reservoir that holds a coolant, an embedded pump, a cooling pad with straps, and long insulated tubes connecting the reservoir to the pad.

Figure 1.1: Examples of cooling systems for home use.

The coolant circulates from the reservoir through the insulated tube to the cooling pad and then back to the reservoir. Coolant typically is water or ice/water mixture depending on how cold the temperature needs to be. There are challenges with those home cooling systems. One is keeping coolant temperature constant during the circulation in a cooling session. Despite the insulation of the tubes, heat from the treatment tissue site would result in razing the coolant temperature. Experimental measurements showed coolant temperature elevations of more than 6°C during a cooling session of 20 minutes with the initial coolant temperature at 8°C [Singh et al., 2022].

Some systems do not have more than one coolant flow speed or more than one setting for controlling the time duration of a cooling session. Another problem is the uncertainty of cold penetration to deep tissue region of surgical sites, as well as how long it takes for the cooling to penetrate the targeted surgical site. In addition, it is possible that extremely low coolant temperatures and/or exceptionally long cooling session may result in whole-body hypothermia (i.e., the body loses heat more than produced) or frostbite on the skin surface (i.e., freezing of the skin and underlying tissues). Another challenge is whether the cooling session is working at all. Patients may become inpatient if no immediate results to reduce pain are noticed or the entire process is not to their convenience. Patients may turn to pain killers like opioids to deal with the pain they experience.

1.2.5 Implications of Opioid Epidemic

Patients relying on pain killers often from its effectiveness to produce immediate results. Unfortunately, most patients could easily get addicted to pain medications such as opioids. Opioid addictions became a worldwide issue in recent years. In the U.S., one saw skyrocketed increase in opioid overdose-related deaths. Since 1990s, opioid prescription was widespread due to the pharmaceutical companies' claim that there had no addicting side effects [National Institute on Drug Abuse 2021]. However, the highly addictive nature of opioids led to a snowball-rolling effect when patients found that they required higher and higher amount of opioid to manage pain. From 1999 to 2019, more than 500,000 people died from overdoses involving opioids that were prescribed or illicitly obtained [CDC 2021]. There have been three waves of opioid overdoses in the U.S. [CDC 2021]. The first wave, starting in the 1990s, was from the increase in

prescriptions of opioids, natural or semi-synthetic [CDC 2021]. The second wave, starting in 2010, involved heroin. The third wave, starting in 2013, was due to manufactured synthetic opioids such as fentanyl [CDC 2021]. In response to the increase in overdoses of opioids and other substances, the National Institute of Health (NIH) with the Department of Health and Human Services (HHS) made efforts to help those patients manage or minimize addiction. Efforts went towards improving treatment and recovery services, providing overdose reversing drugs, advancing better practices for pain management, and other services [National Institute on Drug Abuse 2021]. Unfortunately, all the policies focused on addressing the problem after addiction occurs. Alternative methods to relieve pain in patients before they turn to opioids would have significant impacts on society to fundamentally address opioid addiction. Applying cooling to the surgical site may be a viable solution to this problem.

1.3 Theoretical Simulation of Temperature Field in Tissue

Although experimental measurements of tissue temperatures provide the first-hand data to evaluate effectiveness of those cooling systems, it is not a practical approach to evaluate those systems on patients, especially in the treatment planning stage. Quantitative three-dimensional (3-D) thermal modeling is a powerful tool to help clinicians enhance their ability to deliver safe and effective therapy. Thermal modeling with predicted steady state or transient temperature fields in tissue maximizes the information content of the therapy. It can be used to identify crucial locations to place temperature sensors, evaluate the effectiveness of the treatment methods, and provide feedback information to adjust parameters during a cooling session to either deliver

cooling to targeted regions and/or avoid collateral damage in critical tissue regions [Zhu 2009]. In this study, a mathematic modeling of the temperature field in a human body is used to demonstrate how different combinations of cooling parameters would affect cooling penetration to targeted tissue areas.

Modeling temperature fields in a human body is not straight forward, due to the complicated human vascular system and the enormous number of blood vessels in a human body. It is impossible to model all the thermal interactions between blood vessels and local tissue, using the current computational resources. Typically, there are two approaches in bioheat transfer modeling: vascular modeling and continuum modeling. Vascular modeling approach is to model a blood vessel as a rigid tube buried inside tissue. Vascular modeling proves detailed temperature mapping along blood vessels and its vicinity [Zhu 2009]. However, due to the limitations of available computational resources, one can only include one or two vessels in the tissue domain; blood vessel tapering, and bifurcation are often ignored. On the other hand, in continuum modeling approach, blood vessels are not included in the tissue domain. Its thermal effect is represented by either adding additional terms to the conduction equation or modifying thermal/physical properties. Continuum modeling approach is much simpler to implement than the vascular modeling approach. It is equivalent to solving a partial differential equation if representative parameters related to blood flow are available [Zhu 2009]. However, point-to-point temperature distribution in vessels are not available. Further, the assumptions used to derive these continuum models may not be applied to other tissues and physiological conditions [Zhu 2009].

One of the widely used continuum models is the Pennes bioheat equation [Pennes 1948]. In this model, the thermal effects of local blood profusion in the tissue are modelled as a blood perfusion source/sink term, depending on the local blood perfusion rate and the temperature difference between the local tissue and arterial blood. The tissue domain is often modeled as an isotropic region with fixed thermal/physiological parameters or properties [Manuchehrabadi and Zhu 2017].

Pennes bioheat equation is written as:

$$\rho c \frac{\partial T}{\partial t} = k\nabla^2 T + \omega \rho_b c_b (T_b - T) + Q'''_{met} + Q''' \tag{1.1}$$

where the subscript b refers to blood, local blood profusion rate is ω, T is tissue temperature, k is tissue thermal conductivity, ρ is density, and c is special heat. In this equation, T_b is the arterial temperature and is often assumed equal to 37°C of the normal body core temperature in a human body. The term Q'''_{met} on the right side of Eq. 1.1 is the volumetric heat generation rate due to metabolism, and Q''' is the volumetric heat generation rate by external heating systems such as laser, microwave, nanoparticles, etcetera. Shown in the second term on the right side of Eq. 1.1, the thermal effect of local blood perfusion acts as a heat source when the local tissue temperature T is lower than the arterial temperature T_b, or a heat sink when tissue temperature T is higher than T_b. The blood perfusion rate is defined as the volume of blood supplied to the tissue for oxygen need per unit time and per unit tissue volume. It is an important physiological parameter as it is related to the local oxygen needs and is proportional to the strength of the local blood perfusion source/sink term. In the past three decades, studies have been performed

and demonstrated good agreements between experimental data and theoretical simulation results predicted by the Pennes bioheat equation [Zhu 2009].

1.4 Motivations and Objectives

The above discussion on the limitations of previous studies in the field provides the motivation for the present M.S. thesis research. Body hypothermia is a concern during a cooling session. In thermal neutral situations, the temperature of blood would have the same temperature value leaving from and returning to the heart, resulting in a thermal equilibrium. However, during a cooling session, blood circulates through the body and loses a lot of heat to the cold tissue (see the Pennes bioheat equation) in the vicinity of a cooling pad. Therefore, unless the blood receives heat from other tissue regions, its temperature when returning to the heart would be lower than that when it leaves the heart. This would trigger a spiral decrease in the arterial blood temperature since colder blood would further lower tissue temperature. Previous studies stated that patients feel cold during a cooling session, suggesting possible whole-body hypothermia. However, it is unclear whether whole-body hyperthermia occurs, and the extent of the whole-body hypothermia is also unknown.

In addition, cooling penetration into tissue are often unknown. Evaluation of cooling penetration would lead to identification of cooling parameters to deliver effective cooling at targeted sites while minimizing uncomfortable experiences for patients. The theoretical and experimental study will help clinicians gain a better understanding of the parameters used and how they affect the cooling penetration in the tissue, thus, designing

a safe and effective cooling method that patients can use at home. The data from this study will allow individuals to set cooling parameters, leading to less frustration.

The experiment of this study is performed to collect data of cooling parameters on healthy adult volunteers when applying a cooling pad on the knee. The second part of the study is to simulate temperature fields in a human body to assess cooling penetration in targeted tissue sites during surface cooling. This research attempts to contribute to the on-going investigation of cold therapy. We would like to investigate the resulted temperature field in the leg region under an applied cooling pad, and the roles played by various cooling parameters. To achieve the goals, we design the research to have the following specific aims:

1) To perform experimental studies on healthy adult volunteers to collect cooling parameters during surface cooling on the knee area. Temperatures at the skin site, coolant temperatures in the reservoir at the beginning and end of the cooling session, and temperature mapping of the skin surface would be recorded. In addition, body temperature via a thermometer placed under the tongue will be measured to evaluate whether whole-body hypothermia is induced during the cooling session.

2) To develop a whole-body theoretical model to determine the transient and steady state temperature distributions in a human body during cooling using a skin cooling pad. Physical/thermal parameters will be extracted first based on comparison to the experimental data. Parametric studies will then be conducted to show how various cooling parameters affect the cooling rate and cooling penetration into tissue.

The thesis will be organized into four chapters. Chapter 1 gives the literature review of the research field, limitations of previous studies, motivations of the current study, and specific aims of the research. Experimental methods and theoretical formulations are provided in Chapter 2. Chapter 3 shows the obtained temperature data collected from the experiments and theoretical predictions from the mathematical simulations of temperature fields in tissue near the skin cooling site. Finally, we conclude the thesis with a summary of the research, its contribution to the field, limitations, as well as future works in Chapter 4.

Chapter 2: Methods and Mathematical Formulation

2.1 Experiments

In this part of study, experiments were performed to collect thermal parameters on healthy volunteers during a cooling session via a cooling pad on the knee. The data collected will be used as input to the theoretical model. The experimental procedures of conducting experiments on human volunteers were approved by UMBC Institutional Review Board (IRB) in 2019.

2.1.1 Materials

Experimental materials included a commercially available cooling system, a thermistor bead temperature sensor, and an infrared camera. The commercially available cooling system was an Arctic Ice System Model AIS-2000, which was purchased from Amazon. This cooling system consisted of a reservoir for the coolant (deionized water or water/ice mixture), an embedded pump inside the reservoir, well insulated tubes, and a cooling pad with straps, as shown in Figure 2.1. Once the coolant was flowing to the cooling pad, the water tube bifurcated to cover the entire surface of the cooling pad. During the cooling, a thermistor bead temperature sensor (0.8 mm dia., T-View system, Alpha Technics) was used to measure the interface temperature between the pad and the skin. Considering that the temperature may not be uniform on the interface, a sheet of aluminum foil was placed on the interface of the pad to even out the non-uniformity of the temperature. This would ensure that the temperature reading would not be affected by the location of the temperature sensor on the interface. During the experiment, the cooling pad was wrapped around the volunteer's left knee covering the tissue regions of

both the thigh and leg. Two elastic straps were used to ensure physical contact between the pad and the skin surface. The cooling pad only covered the front half of the knee surface area, shown in Figure 2.1.

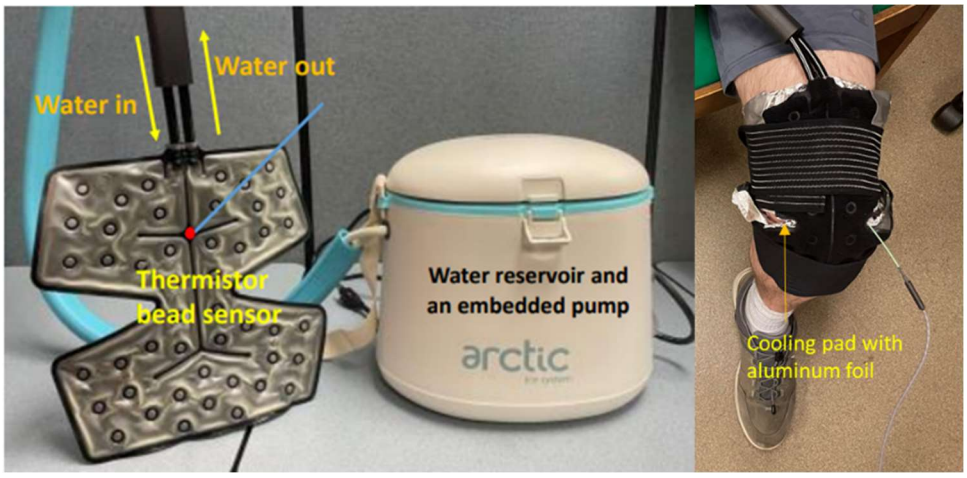

Figure 2.1: Cooling system (left) and cooling pad with aluminum foil (right).

A thermistor is a type of temperature sensor that is made from a ceramic-like semiconductor, such as metal oxides of manganese, nickel, cobalt, copper, iron, and titanium. The semiconductor is then pressed to form a bead, a disk, or cylinder. It is then encapsulated with an impermeable material such as epoxy or glass [Sensor Scientific 2019]. The electrical resistance of the semiconductor is overly sensitive to temperature, allowing the thermistor bead to serve as a temperature measurement sensor. In this study, a thermistor bead with a nominal resolution of 0.001°C was used to record the temperatures throughout the experiment, shown in Figure 2.2 [Vesnovsky et al., 2019]. In conjunction with a computer software provided by the company, the measured temperatures could be displayed on a computer screen and temperature was measured at a high frequency of 7 times/second, and temperature and time data could be saved in the

computer for later analyses. Shown in Figure 2.1, during the cooling session, the thermistor bead was placed at the center of the cooling pad on the thigh region to measure the interface temperature during the cooling session. In addition, the same thermistor bead sensor was used to record the oral temperature of the volunteer before and after the cooling session via being inserted inside a disposal sheath and placed under the tongue of the volunteer. The recording of the oral temperature lasted two minutes that were determined as sufficiently long to reach thermal equilibrium in the mouth [Vesnovsky et al., 2019]. The coolant temperature in the reservoir was also measured using the thermistor bead sensor before and after the cooling session, as well as the air temperature in the room. Repeatedly using the same thermistor bead sensor minimized measurement errors due to variations among temperature sensors.

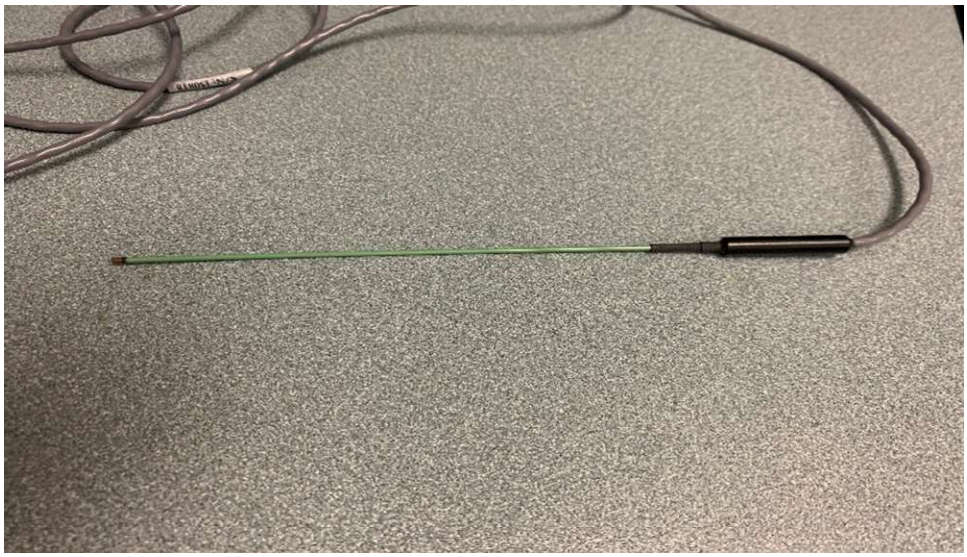

Figure 2.2: The thermistor bead temperature sensor used in the experiment.

A TIS45 Fluke Corporation infrared camera with SmartView Classic thermal imaging software (Fluke Cooperation, Everett, WA) was used to record the temperature

of the targeted skin area before and after the cooling session [Li et al., 2016]. Shown in Figure 2.3, the non-invasive infrared camera allowed temperature mapping of the entire skin area before a cooling session (the left panel) and after a cooling session (the right panel). Temperature recovered very quickly after the end of the cooling session, therefore, temperature contours in the right panel of Figure 2.3 should be much higher than the temperatures during the cooling. In addition, the accuracy of the infrared camera is unknown in this study, due to the unavailable value of the total hemispheric emissivity of the skin surface. It is well known that emissivity of human skin varies from 0.92-0.99, despite a wide range of skin tones [Charlton et al., 2020; Li et al., 2016]. However, setting the emissivity value from the lower limit to the upper limit would still result in an uncertainty of more than 1°C in the temperature readings.

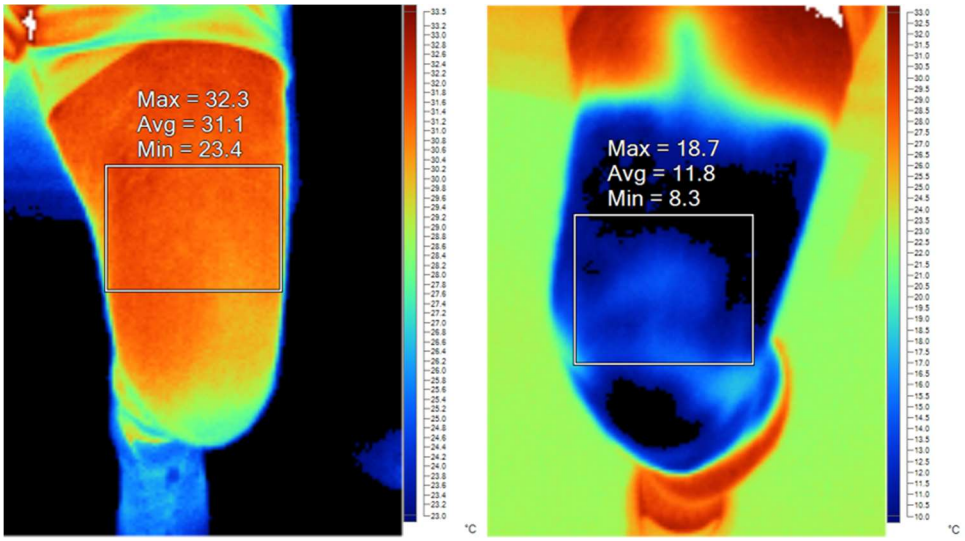

Figure 2.3: Infrared image of the knee region.

2.1.2 Experimental Procedures

Three healthy human volunteers were recruited to this study from the University of Maryland Baltimore County in compliance with local IRB approval. On the day of the

experiment, the volunteer wore shorts and sits comfortably in a laboratory. Water or ice/water mixture was placed into the reservoir of the cooling system. Preliminary studies demonstrated rising temperature of water of more than 6°C during the cooling session, if no ice was added to the reservoir [Singh et al., 2022]. However, temperature elevation was only 1-2°C if an ice/water mixture was used as the coolant, resulting in a relatively constant coolant temperature during the cooling session. While waiting for the thermal equilibrium inside the reservoir, the oral temperature of the volunteer was measured first. Then, the infrared camera was used to take the infrared image of the skin surface near the left knee. Finally, the prepared cooling pad was wrapped tightly on the volunteer's left knee, like that shown in Figure 2.1. The pump was turned on and the cooling lasted for 20 minutes. After the cooling session ended, the cooling pad was removed. The skin temperature mapping was taken again by the infrared camera. The thermistor bead again recorded the volunteer's oral temperature and the temperature of the coolant in the reservoir.

2.2 Theoretical Modeling of Temperature Field in a Human Body

Theoretical simulations were conducted after the experiments using a commercially available finite element method software COMSOL. Both the transient and steady state temperatures were obtained. The software allows adjusting various parameters and properties. The simulations were conducted to first extract the unknown lumped heat transfer coefficient h_{water}, which is related to the overall thermal resistance between the coolant (water) and the skin surface, based on the measured skin

temperatures in the experiments. Then, parametric studies were performed to evaluate various parameters on the cooling penetration in tissue.

2.2.1 Model Formulation

Simulations started with generating a human body model based on measured size and geometry of a human volunteer. As shown in Figure 2.4, the model consisted of three major components: the brain, the internal organs, and the muscles. Each component had its own uniform thermal properties and physiological parameters. For simplicity, all the tissue regions other than the brain or internal organs were modeled as muscle, without including skin, fat, or bones. The cooling pad was placed on the knee region. The cooling pad covered the front half of the surface area of the knee, as shown by the blue region in Figure 2.4, like that in the experiments.

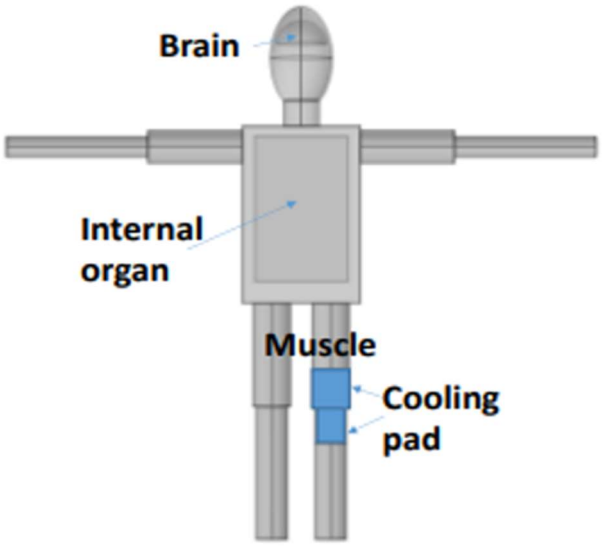

Figure 2.4: COMSOL model of a human body with a cooling pad attached to the knee area.

The Pennes bioheat equation [Pennes 1948] was used for simulating the temperature fields of the body as:

$$\rho_t c_t \frac{\partial T_t}{\partial t} = k_t \nabla^2 T_t + \omega \rho_b c_b (T_b - T_t) + Q'''_{met,t} \quad (2.1)$$

In Eq. 2.1, ρ is density, c is specific heat, k is thermal conductivity, ω is local blood perfusion rate, and $Q'''_{met,t}$ is the volumetric heat generation rate due to metabolism. Subscripts t and b represent tissue and blood, respectively. Typically, a person wears clothes to maintain a thermal equilibrium with her/his surroundings. In this study, the cloth is removed, and the naked body was exposed to an ambient environment, and the thermal resistances due to convection/radiation with the air were lumped as an overall heat transfer coefficient $h_{air.}$ The water flows through the tubes on the cooling pad, and it was separated from the skin surface by a plastic layer and a very thin aluminum sheet. Therefore, the boundary condition of the cooling pad was also lumped as an overall heat transfer coefficient h_{water} [Singh et al., 2020]. Mathematical expression of the boundary conditions is described by the following equations:

$$-k \frac{\partial T_t}{\partial n}\Big|_s = h_{water}(T_t - T_{water}) \quad \text{at the cooling surface} \quad (2.2)$$

$$-k_t \frac{\partial T_t}{\partial n}\Big|_s = h_{air}(T_t - T_{air}) \quad \text{at the rest of the body surface} \quad (2.3)$$

Table 2.1: Physical and physiological properties

Properties	Brain	Internal Organs	Muscle	Blood
$k, W/mK$	0.52	0.52	0.52	0.50
$\rho, kg/m^3$	1060	1060	1060	1060
$c, J/kgK$	4186	4186	4186	4186
$\omega_0, 1/s$	0.009	0.0021	0.00053	
$Q'''_{met,0}, W/m^3$	9225	2459.7	553.5	

Physical properties and physiological parameters are needed in the model and are given in Table 2.1. Physical properties of tissue were like that of water, as tissue is approximately 75% of water. One notes that the metabolic heat generation rate and blood perfusion rate were the baseline values before the cooling. It is well known that local blood perfusion rate usually decreases as temperature drops, and it has a well know relationship shown as follows [Diao et al., 2003]:

$$\omega = \omega_0 3^{(T_t-37)/10} \tag{2.4}$$

This above equation was applied only to the knee regions under the cooling pad. This is a protective mechanism of the human body to prevent substantial amounts of heat loss from the body in a cold environment via vasoconstriction of blood vessels. It suggests that when the local temperature decreases by 10°C, the local blood perfusion rate decreases to 1/3 of its baseline value before the cooling. Note that the value "3" was based on some experimental data. However, some other researchers used the value of "2" in the above equation, implying that ω decreases to ½ of its baseline value after temperature reduction of 10°C [Abramson et al., 1958; Diao et al., 2003; Hoffman et al., 1982; Smith and Zhu 2010].

Normally, local metabolic heat generation rate Q'''_{met} is coupled with local blood perfusion rate since the primary function of blood flow is to provide oxygen to tissue. Therefore, in the study, the coupled relationship was assumed to be valid during the cooling, leading to the following relationship between Q'''_{met} and local temperature as:

$$Q'''_{met} = Q'''_{met,0} 3^{(T_t - 37)/10} \tag{2.5}$$

2.2.2 Finite Element Method Software

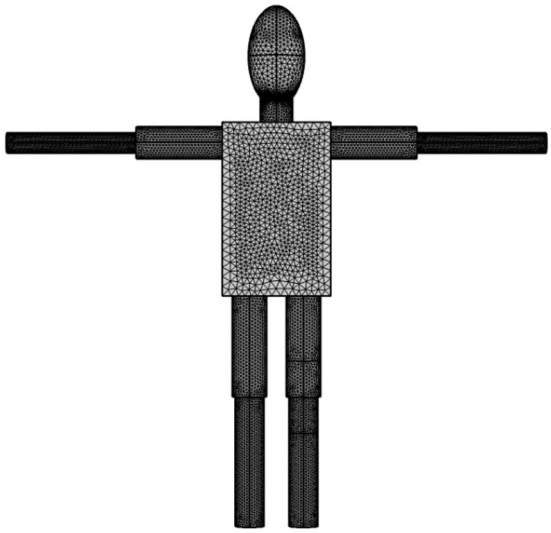

Figure 2.5: Whole body model with generated meshes.

A commercially available finite element software COMSOL was used to simulate the temperature fields. Figure 2.5 shows the overall meshing of the entire simulation domain. In this study, our focus was on the knee region with the cooling pad. Sensitivity to the mesh size was checked on the thermistor bead location in the cooling region. Specifically, the mesh size setting at the knee regions was changed to increase the total number of elements to determine if changing the mesh size would impact the temperature

field. Shown in Table 2.2, when the total number of elements was more than doubled from 12,277 to 31,597, the predicted maximal, minimal, and average temperatures at the skin location after 20 minutes of cooling resulted in variations of less than 1% in the temperature values. The mesh in the rest of the body was also adjusted via doubling the total number of the elements. One found less than 0.1% in the predicted temperature at the thermistor bead location.

Table 2.2: Sensitivity of simulated temperature results on the mesh size in the knee region

Mesh	No. of Elements	T_{max}, °C	T_{min}, °C	T_{avg}, °C
Mesh 1	5,415	33.294	5.0528	19.1935
Mesh 2	12,277	33.292	5.3345	19.3133
Mesh 3	31,597	33.292	5.3766	19.334

2.2.3 Simulation Procedures

First, we the calculated the overall heat transfer coefficient of air surrounding the human volunteer, assuming a free convection over a horizontal cylinder and a radiation heat loss to a cold environment using the Stefan-Boltzmann's law. This lumped h_{air} was applied to the rest of the surfaces of the body. Then the simulation was conducted using the average coolant temperature during a cooling session in the experiment to extract the overall heat transfer coefficient of the coolant. The value of the overall heat transfer coefficient at the cooling pad h_{water} was continuously adjusted until the predicted skin temperature matched the experimental measurement at the thermistor bead site 20 minutes after the cooling. The value of h_{water} was finalized when the absolute value of the deviation was less than 0.1°C. Finally, parametric studies were performed to examine the coolant temperature (0 - 20°C) and the overall heat transfer coefficient of the coolant (20

- 200 W/m^2K) on the temperature fields. In the transient heat transfer simulations, the steady state temperature field before the cooling was used as the initial condition of the transient simulations on cooling penetration in the tissue region near the knee.

Chapter 3: Results

3.1 Lumped Heat Transfer Coefficient h_{water}

In this study, the skin was exposed to a cold environment such as the floor, the walls, and the ceilings to exchange radiation, and it might lose heat to the frigid air surrounding the body via free convection. Since the convection heat loss and radiation heat loss occurred concurrently, in this study, a lumped heat transfer coefficient h_{air} was used to include the combined heat transfer rates from both mechanisms. Shown in Eq. 3.1, the total heat transfer rate from the skin surface of a body is described by the Newton's law of cooling and the Stefan-Boltzmann's law.

$$q = q_{conv} + q_{rad} = h_{conv}A(T_s - T_{air}) + h_{rad}A(T_s - T_{sur}) \qquad (3.1)$$

In Eq. 3.1, q is heat transfer rate, A is surface area, T_s is the surface temperature of the body, *and* h_{conv} is the convection coefficient due to free convection to the surrounding air when the motion of air is triggered by buoyance-related forces. h_{rad} in Eq. 3.1 is an equivalent heat transfer coefficient due to radiation to the surrounding environment. Based on the Stefan-Boltzmann's law describing radiation heat exchange between a gray and diffuse surface (the human body) and its surrounding, the heat transfer coefficient due to radiation is given as [Kosky et al., 2020]:

$$h_{rad} = \varepsilon\sigma(T_s - T_{sur})(T_s^2 + T_{sur}^2) \qquad (3.2)$$

where ε is the total hemispherical emissivity of the skin, and σ is the Stefan-Boltzmann's constant equal to $5.67*10^{-8}$ W/m^2 K. On can combine the two-heat transfer mechanisms together when assuming $T_{air} = T_{sur}$, leading to a lumped overall heat transfer coefficient h_{air} [Bergman et al., 2011]:

$$q = h_{air}A(T_s - T_{air}), and\ h_{air} = h_{conv} + h_{rad} \quad (3.3)$$

Since the focus of this study is the temperature field in the knee area, h_{conv} was estimated from free convection heat transfer occurring between a horizontal cylinder (the thigh when the volunteer was in sitting) and its surrounding moving air. In this study, it was assumed that the cylinder was in a uniform temperature as measured by the infrared camera. The dimensionless parameter (the average Nusselt number, *Nu*) should be a function of the dimensionless Rayleigh's number (*Ra*), shown in the following equation [Bergman et al., 2011]:

$$\overline{Nu}_D = \frac{\overline{h_{conv}}D}{k} = CRa_D^n \quad (3.4)$$

where *C* and *n* were determined by the range of the calculated Rayleigh's number. In Eq. 3.4, *D* is the diameter of the thigh of the volunteer as 0.12134 m. Assuming T_{air} = 22°C, T_s = 31°C, the gravitational constant *g* as 9.8 m/s^2, thermal diffusivity of air α = $22.5*10^{-6}$ m^2/s, kinematic viscosity of air ν = $15.89*10^{-6}$ m^2/s, and thermal expansion coefficient of air β = 1/300 K^{-1}, the Rayleigh's number Ra_D was calculated as:

$$Ra_D = \frac{g\beta(T_s - T_{air})}{\alpha\nu} = \frac{9.8*\left(\frac{1}{300}\right)*(31-22)}{22.5*10^{-6}*15.89*10^{-6}} = 1.469 * 10^6 \quad (3.5)$$

Based on the correlation provided in the textbook by Bergman [Bergman et al., 2011], the coefficients in Eq. 3.4 were determined as:

$$C = 0.480, n = 0.25 \quad (3.6)$$

The average Nusselt number $\overline{Nu_D}$ was then calculated as 16.71, leading to the determination of the free convection coefficient h_{conv} as 3.6 W/m^2 K.

In the meantime, the equivalent heat transfer coefficient due to radiation was calculated as:

$$h_{rad} = \varepsilon\sigma(T_s + T_{sur})(T_s^2 - T_{sur}^2)$$
$$= 0.98 * 5.67 * 10^{-8}(31 + 273 + 22 + 273) * [(31 + 273)^2 + (22 + 273)^2]$$
$$= 5.97\ W/m^2K \quad (3.7)$$

After obtaining both *h* values, one could lump them together as:

$$h_{air} = h_{conv} + h_{rad} = 9.57\ W/m^2K \quad (3.8)$$

Although the lumped heat transfer coefficient may vary from one skin surface to another, in this study, the coefficient remains constant at 9.57 W/m^2 K over other surfaces of the body.

3.2 Experimental Data

The room temperature was found to not change significantly from day to day, it was around 22°C, shown in Table 3.1. The coolant temperature before the cooling session was close to 0°C as ice-water mixture was placed inside the reservoir. However, after the cooling session, the coolant temperature increased slightly by approximately 1°C, shown in Table 3.1. The infrared camera was used to record the body temperature. When the total hemispherical emissivity was selected as 0.94, the infrared camera measured temperature at the center of the thigh surface was around 31°C.

Table 3.1: Recorded data of room temperature, water temperature and body temperature before and after the cooling, average skin temperature of the thigh before the cooling by the infrared camera

	Volunteer 1	Volunteer 2	Volunteer 3
T_{air}, °C	22.0	22.0	22.1
T_{water} (before), °C	0	1.36	0.3
T_{water} (after), °C	1.36	2.32	0.99
T_{body} (before), °C	36.7	36.4	36.9
T_{body} (after), °C	36.8	36.7	37.2
T_{skin} by infrared, °C	31.1	31.3	31.4

All volunteers felt cold sensation under the cooling pad. The cooling was uncomfortable to the volunteers, however, tolerable. The volunteers commented that a cooling duration less than 20 minutes was the length they would tolerant. After the cooling, the skin surface showed reddish color due to the temperature reduction. Follow-ups with the volunteers did not show sustained damage to the skin surface, as the skin surface under the pad returned to their normal tone several hours after the cooling session.

The body temperatures measured before the cooling experiment were 36.4°C - 36.9°C. Despite the cooling session, all volunteers' body temperatures increased slightly by approximately 0.1-0.3°C. This increase may be due to the sensitivity of the thermistor bead sensor and/or uncertainty of its location under the tongue. However, one thing is clear from the experiments that no systemic whole-body hypothermia occurred after 20 minutes of cooling on the knee using the cooling pad. Cold sensation experienced by all volunteers was not a reliable indication of systemic hypothermia in the body.

Table 3.2: Recorded skin temperatures during a cooling session of 20 minutes

Time, minutes	Volunteer 1, °C	Volunteer 2, °C	Volunteer 3, °C
0	26	27.53	26.285
1	16.49	17.31	9.673
2	12.80	15.40	8.351
3	12	13.84	7.401
4	10.98	12.82	6.6
5	10.17	11.97	6.094
6	9.33	11.35	5.655
7	8.59	10.81	5.287
8	8.06	10.35	4.986
9	7.715	9.98	4.736
10	7.34	9.67	4.540
11	6.96	9.36	4.355
12	6.48	9.16	4.235
13	6.28	8.95	4.077
14	6.07	8.76	3.973
15	5.85	8.63	3.865
16	5.67	8.47	3.793
17	5.56	8.34	3.715
18	5.43	8.23	3.646
19	5.35	8.12	3.584
20	5.24	8.02	3.571

In addition, the temperature transients at the skin surface were recorded by the thermistor bead sensor under the cooling pad. Shown in Table 3.2, the skin temperature was recorded every minute for the entire cooling duration of 20 minutes. Although the

skin temperature before placing the cooling pad was around 33°C, one notes that its initial temperature was around 26°C after placing the cooling pad, however, before turning on the coolant circulation. This may be due to the changes in the boundary condition via placing a room-temperature cooling pad on the skin surface.

Right after cooling for 1 minute, the temperatures dropped to 9-17°C, varying significantly from one person to another. 5 minutes later, the temperatures decreased to 6.6°C - 12°C. At the end of the cooling session of 20 minutes, the temperature varied from 3.6°C to 8°C. Despite similar coolant temperatures in the experiments for the volunteers, individual human volunteers showed different temperature dropping rates, as well as different ending temperatures after 20 minutes. It also demonstrated that it was unlikely that steady state was established after 20 minutes. Temperature would have continuously dropped if the cooling sessions were longer.

3.3 Simulation Results

To find the temperature field on the human body model during a cooling session, both steady state and transient heat transfer simulations are needed. Steady state heat transfer simulation was conducted first to determine the temperature field of the whole body without the cooling pad present. Transient simulations were then conducted with the cooling pad present and the simulations was conducted for 20-30 minutes, to see temperature change over time. The h_{water} was determined by comparing predicted temperatures after 20 minutes to the recorded temperatures in the experiments.

3.3.1 Steady State Temperature Field before the Cooling

The steady-state simulation was performed first to predict the temperature field of the human body without the cooling pad. The overall heat transfer coefficient over the entire body was 9.57 W/m^2 K, and the blood perfusion rate and metabolism values are shown in Table 2.1, and they did not depend on local tissue temperature. Shown in Figure 2.4, the boundary condition at the cooling pad location was replaced by the free convection of Eq. 2.3. Figure 3.1 illustrates the temperature contours of a central slice of the body. One notes that the maximal temperature occurs at the center of the brain tissue and the internal organ region, approximately 37.3°C. This is 0.3°C higher than the prescribed arterial temperature of 37°C which is consistent with experimental data of medical literature of previous studies [Bartgis et al., 2016], due to the large metabolic heat generation rate in both tissue regions. On the contrary, the rest of the body tissue has temperatures much lower than 37°C. The minimal temperature of 32°C occurs at the fingertips or toes, consistent of a typical experience for a person. The low temperatures at the extremities are primarily due to their large ratio of surface area to volume, as well as low metabolic heat generation rate under resting conditions. From the simulation, one can see an average temperature at the thigh area near the knee as 33.12°C. This temperature is close to the range of the measured temperature at the skin surface of the thigh by the infrared camera. The uncertainties of the unknown emissivity and baseline blood perfusion rate add difficulty to evaluate the accuracy of the infrared data. However, comparison between the model predictions and experimental measurements may be suitable for extracting properties in the future.

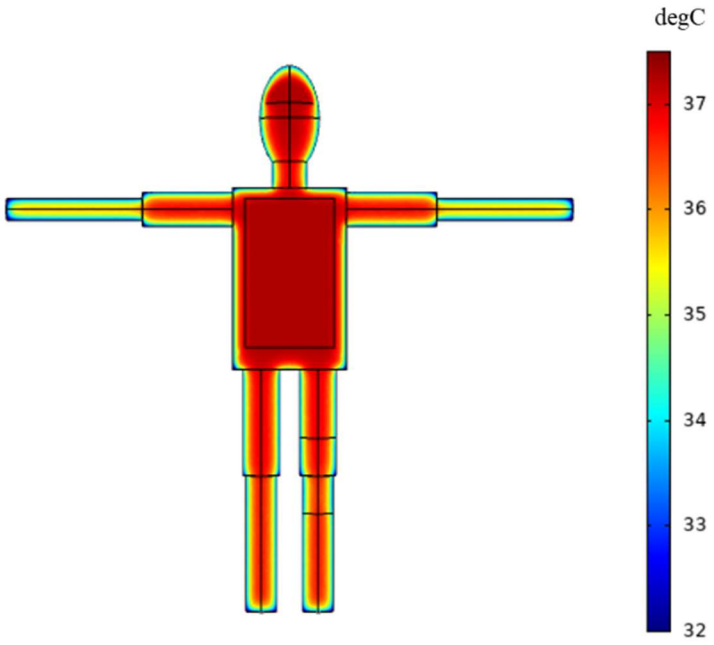

Figure 3.1: Temperature contours of the central cross-sectional plane of the body before the cooling initiation.

3.3.2 Transient Simulations for Extracting the Overall Heat Transfer Coefficient, h_{water}

The lumped overall heat transfer coefficient h_{water} is difficult to derive, due to the unknown materials of the plastic tubes of the cooling pad and the aluminum sheet, as well as the difficulty to derive the velocity field of the circulating water. In this study, transient heat transfer simulations were conducted based on the recorded average water temperatures during the cooling (Table 3.1) and the geometry of the thigh of the volunteer. The simulations started with an assumed value of h_{water} to predict the temperature's decay curve at the center location of the thigh skin surface under the pad. For simplicity, only the temperature value at the location after 20 minutes of cooling was matched. The value of h_{water} was adjusted until the absolute value of the difference between the experimental measurement and theoretical prediction was less than 0.1°C.

Table 3.3 gives the comparisons between the experimental data and simulated results of the three volunteers. The extracted overall heat transfer coefficient h_{water} varied from 116 to 248 W/m^2 K. Although in theory the overall heat transfer coefficient should be the same among volunteers, the large variation from one volunteer to another may suggest that some thermal resistances should be counted in the simulations. For example, the physical contact between the pad and skin surface was ensured by the elastic wrap. However, one may not be 100% sure that conduction resistances due to air between the pad and the skin was the same among the volunteers. Although an aluminum foil was used to even out the non-uniformity of temperature on the pad surface, the uncertainty of the temperature sensor location might also contribute to the variations of the extracted h_{water} value. Another plausible reason for the variation in h_{water} is due to the uncertainty of the baseline blood perfusion rate and metabolism. In this study, they were assumed the same for all volunteers, however, they may be different from one volunteer to another.

Table 3.3: Experimental measurements and simulation result at the sensor location after surface cooling of 20 minutes, and extracted value of h_{water} of the three volunteers

	h_{water}, W/m^2 K	Experiment Measurement	Simulation Result
Volunteer 1	160	5.24°C	5.34°C
Volunteer 2	116	8.02°C	8.01°C
Volunteer 3	248	3.57°C	3.59°C

Figure 3.2 compares the experimental measurements by the thermistor bead (symbols) and theoretical predictions (curves) at the same skin location, using the finalized overall heat transfer coefficient h_{water} of each volunteer. Although the match was achieved at the time instant of 20 minutes, one can see overall good agreement over most

of the cooling session, except during the initial few minutes. Continuous cooling to 30 minutes illustrates further temperature reduction at the skin surface. Further temperature drop at the skin surface is less than 1°C, and a steady state would be established soon.

Cooling penetration to deep tissue under the skin pad is illustrated by the temperature contours of the central cross-section of the thigh and leg area in Figure 3.3. The dark blue region in Figure 3.3 indicates significant temperature reduction in the tissue region under the cooling pad (~5°C) seen on the front side of the knee region. However, the temperature field on the rear side of the knee region is almost the same as its pre-cooling field, unaffected by the cooling pad.

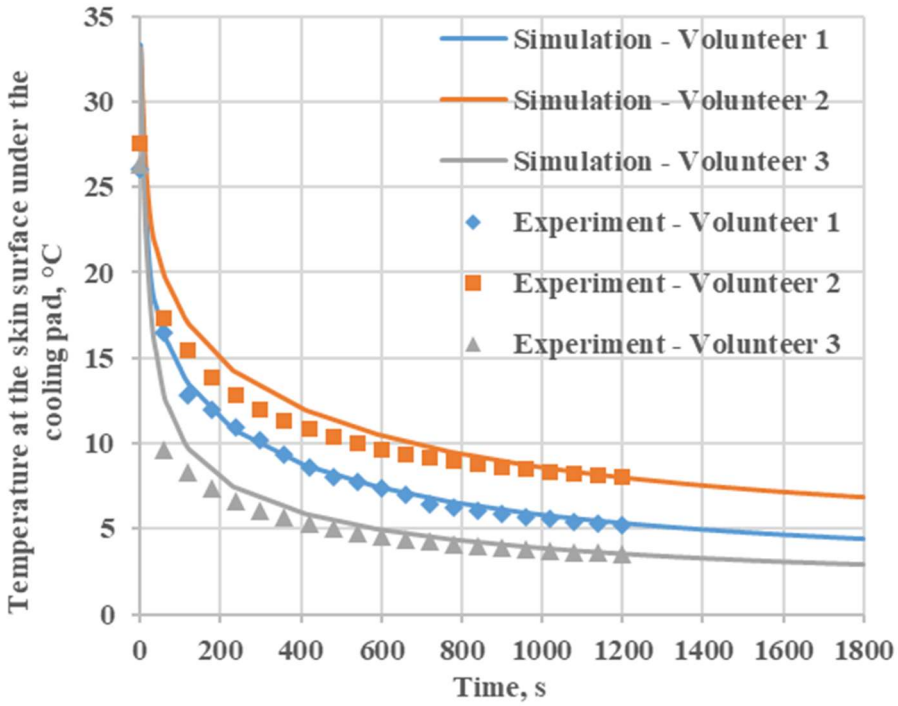

Figure 3.2: Recorded temperatures by the thermistor bead (symbols) and simulation predictions with the finalized h_{water} (curves) at the skin location during a cooling session.

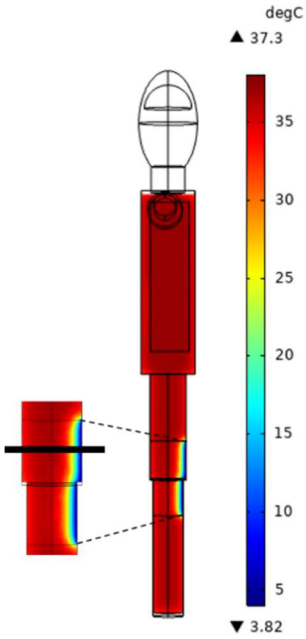

Figure 3.3: Temperature contours of the central cross-sectional plane of the thigh and leg region after cooling of 30 minutes.

3.4 Parametric Study of Effects of Cooling Parameters on the Temperature Field

Parametric studies were conducted to evaluate the effects of various cooling parameters on the temperature field in the knee area and the resulted cooling penetration. In this study, the parametric study was performed based on the physical model of one volunteer. Cooling parameters include the water temperature and the overall heat transfer coefficient of water. The simulation time was selected as 20 minutes based on the experimental observations that it was the longest time the volunteers could tolerate.

3.4.1 Effect of T_{water} on the Temperature Field

For in-home use of commercially available cooling systems, the water temperature may be changed due to the coolant. One can directly use tap water, or ice/water mixture. In this parametric study, five coolant temperatures (0, 5, 10, 15, and

20°C) were evaluated. The value of h_{water} was selected as 160 W/m^2 K from that of volunteer #1.

The transient temperature distribution along the horizontal line in Figure 3.3 is plotted in Figure 3.4. The results show a relatively uniform temperature distribution inside the thigh before the cooling, varying from ~33°C at the skin to 37°C at the center. The top panel of Figure 3.4 gives the temperature profile when the coolant is 0°C circulating in the cooling pad. It shows that temperatures decreases rapidly due to cooling, especially during the first five minutes. After 20 minutes of cooling, skin temperature decreases to approximately 4°C. One notes that the temperature profile in the tissue does not change very much after cooling for 15 minutes. The bottom panel of Figure 3.4 illustrates the temperature decay inside the tissue with the coolant temperature at 20°C. Contrary to the large temperature reduction in the top panel, temperature decreases are limited by the coolant temperature. After cooling 20 minutes, the skin temperature reduces to approximately 22.5°C.

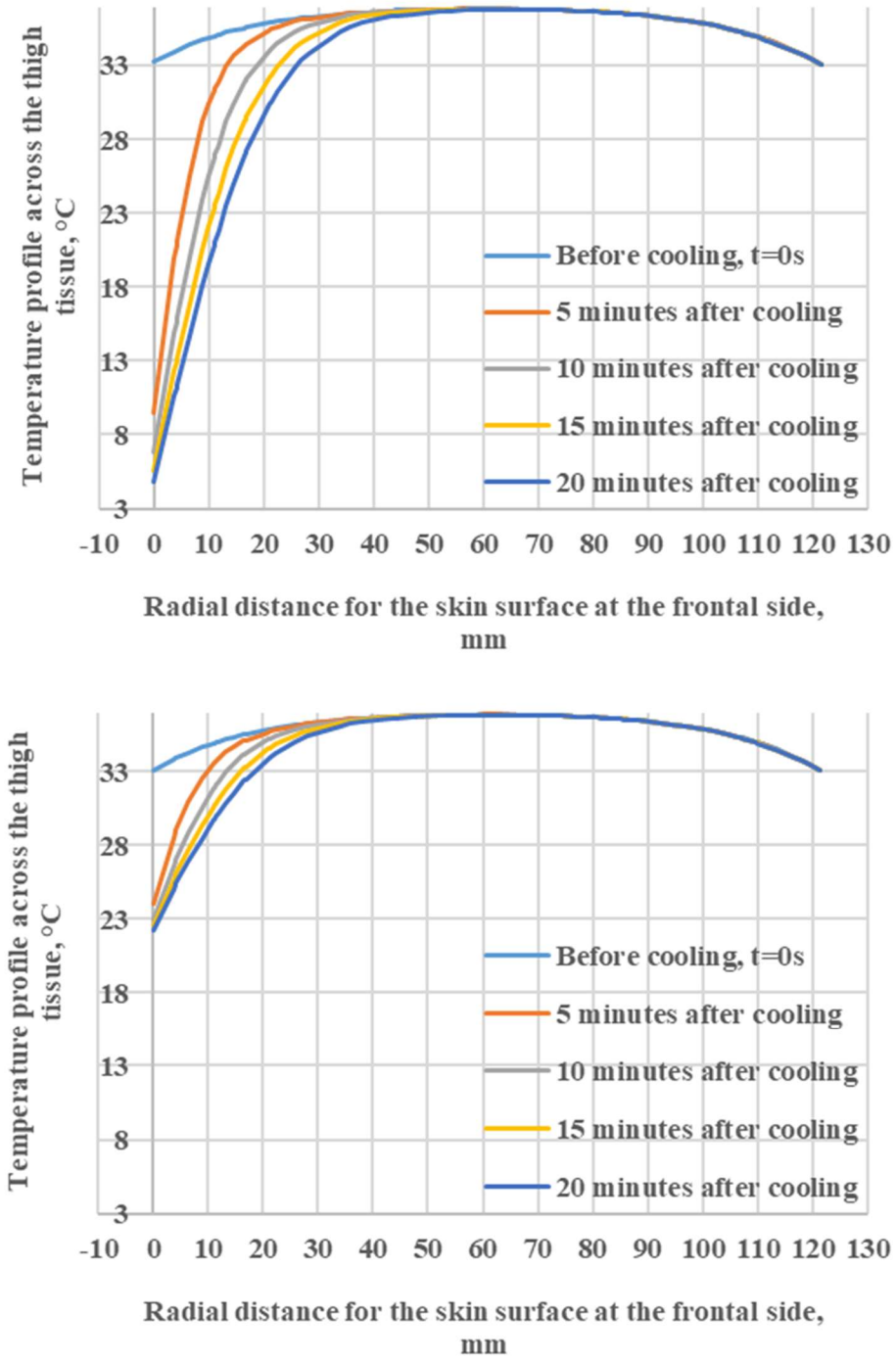

Figure 3.4: Temperature profile across the thigh tissue (the horizontal line in Figure 3.3) at various time instants during the cooling. The top panel is for coolant temperature at 0°C and the bottom panel is for coolant temperature at 20°C.

The goal of most in-home cooling systems is to reduce temperature of the deep tissue at the targeted region, not on the skin surface. Cooling penetration depth was defined as the vertical distance between the skin surface and the tissue location at a specific threshold temperature. In this study, the estimated penetration depth based on the tissue temperature profile along the horizontal line is shown in Figure 3.3.

It is not clear which critical, or threshold tissue temperature should be used to achieve local pain relief. In this study, we evaluate the penetration depth based on a threshold tissue temperature from 25°C to 35°C. The cooling penetration depth with a threshold of 35°C would be much bigger than that with a threshold of 25°C. Figure 3.5 plots the trends of the cooling penetration depth affected by the value of the threshold temperature, and its dependence on the coolant temperature. The upper limit of the threshold temperature is assumed as 35°C. Under this threshold, the penetration depth would have a maximal value of 33 mm when the coolant temperature is 0°C and a minimal value of 26 mm when the coolant temperature is 20°C. If the targeted tissue region requires a much bigger temperature reduction, the cooling penetration decreases significantly. When the coolant temperature is 0°C, the maximal penetration depth decreases from 33 mm to 25 mm, and finally to 14 mm, when the threshold temperature is selected from 35°C to 33°C, and to 25°C, respectively. Increases in the coolant temperature from 0°C to 20°C would significantly reduce the penetration depth by 21% when the threshold is selected as 35°C, or 72% when the threshold is selected as 25°C. For patients who prefer to use tap water at 20°C, cooling can penetrate deep tissue up to 26 mm when the threshold is selected as 35°C. This coolant temperature of 20°C is still beneficial to patients if the surgical site is within 26 mm from the skin surface.

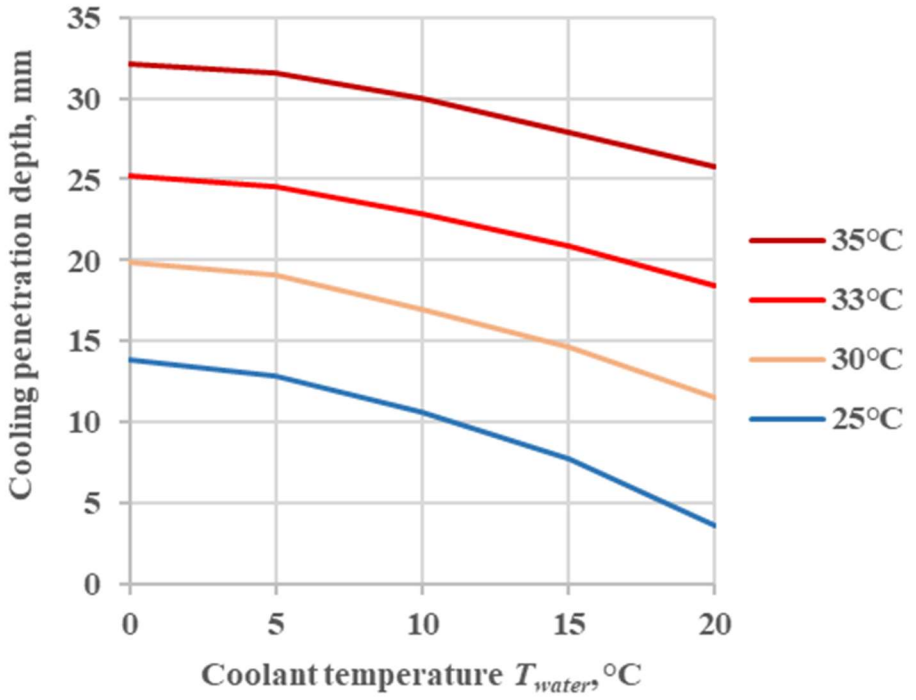

Figure 3.5: Effects of the coolant temperature T_w on the cooling penetration depth after cooling of 20 minutes under a specific threshold temperature (25°C, 30°C, 33°C, or 35°C).

3.4.2 Effect of h_{water} on the Temperature Field

It is well known that the overall heat transfer coefficient h_{water} reflects the thermal resistance between the water and the skin surface. Based on the Newton's law of cooling, the thermal resistant is inversely proportional to h_{water}. Therefore, the resulted skin temperature would be directly affected by the value of h_{water}. Due to the broad range of the extracted h_{water} values among the three volunteers, we would like to examine how sensitive the resulted temperature field is to the value of h_{water}. In this study, h_{water} was selected as 20 W/m^2 K, 40 W/m^2 K, 80 W/m^2 K, 120 W/m^2 K, 160 W/m^2 K, and 200 W/m^2 K. This range was chosen based on our understanding of the normal range of

convection coefficient of liquid (100-20000 W/m^2 K) [Bergman et al., 2011]. The lower limit of 20 W/m^2 K in this study was based on added conduction resistances due to the plastic sheet and the aluminum sheet. The added conduction resistances would lead to a decrease from the lower limit of the overall heat transfer coefficient of 100 W/m^2 K. The upper limit of 200 W/m^2 K in this study was selected due to our understanding that a larger h_{water} would not change the temperature field significantly, as discussed later. All the simulations were conducted assuming that T_{water} = 0°C.

Figure 3.6 shows the temperature distribution along the horizontal line at various time instants, when h_{water} is chosen as 20 W/m^2 K (the top panel) or 200 W/m^2 K (the bottom panel). A larger overall heat transfer coefficient implies a smaller thermal resistance between the water and the skin, resulting in a skin temperature closer to the water temperature. When h_{water} is selected as 20 W/m^2 K, the skin temperature decreases from the baseline of 33°C to 22°C after cooling for 20 minutes. However, the skin temperature is much lower when h_{water} is selected as 200 W/m^2 K, and it decreases to 4°C after cooling for 20 minutes, a temperature that is much closer to the coolant temperature of 0°C.

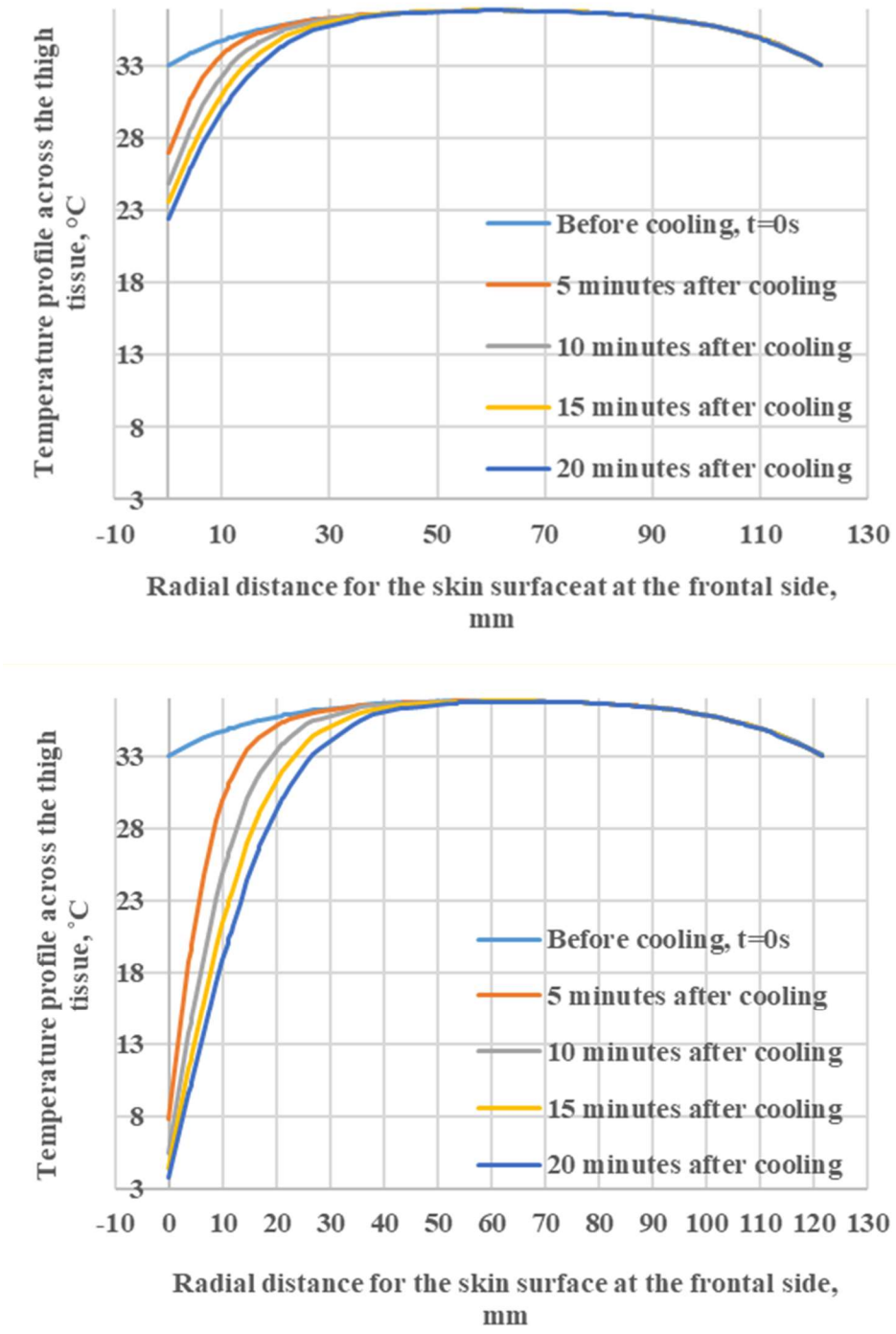

Figure 3.6: Temperature profile across the thigh tissue (the horizontal line in Figure 3.3) at various time instants during the cooling. The top panel is for h_{water} = 20 W/m^2 K, and the bottom panel is for h_{water} = 200 W/m^2 K.

It is difficult to see the trend of cooling penetration depth from Figure 3.6. Instead, the dependence of cooling penetration depth on the value of h_{water} is illustrated in Figure 3.7. Again, one notes how the penetration depth is bigger when the selected temperature threshold is larger. When h_{water} is 200 W/m^2 K, the penetration depth increases from 15 mm with the threshold of 25°C to 34 mm with the threshold of 35°C. The penetration depth affected by the h_{water} value shows a positive trend with the h_{water} value. When the threshold is selected as 35°C, the penetration depth increases from 24 mm to 34 mm (by 41%) over the entire range of h_{water}, while it increases by 53% with the threshold temperature as 33°C.

All the curves in Figure 3.7 demonstrated that the penetration depth is sensitive to the h_{water} value in the range of h_{water} < 120 W/m^2 K. Shown in Figure 3.7, the penetration depth with the threshold temperature at 35°C, increases from 24 mm when h_{water} =20 W/m^2 K, to 32 mm when h_{water} = 120 W/m^2 K. Once h_{water} is larger than 120 W/m^2 K, the penetration depth still increases with the h_{water} value. However, the increase is very minor. Shown in Figure 3.7, increasing the h_{water} value from 120 to 200 W/m^2 K only results in a further increase in cooling penetration depth by less than 2 mm in tissue, i.e., from 32 mm to 34 mm. Based on the trends shown in Figure 3.7, one would not expect further significant increases in the cooling penetration when the h_{water} value is larger than 200 W/m^2 K.

This result is expected due to the combined thermal resistance from the coolant to deep tissue location. Using a quite simple thermal resistance analyses, one can see that the total thermal resistance between the coolant and deep tissue consists of a convection resistant and a conduction resistance in a series arrangement. Once the value of h_{water} is

exceptionally large, the contribution of the convection resistance is much less important than the conduction resistance of the tissue. Therefore, further increases of h_{water} would only affect the skin temperature, however, it has a very minor influence on the temperature field in the deep tissue. Therefore, this would lead to the insensitivity of the cooling penetration depth on the h_{water} value when h_{water} is exceptionally large.

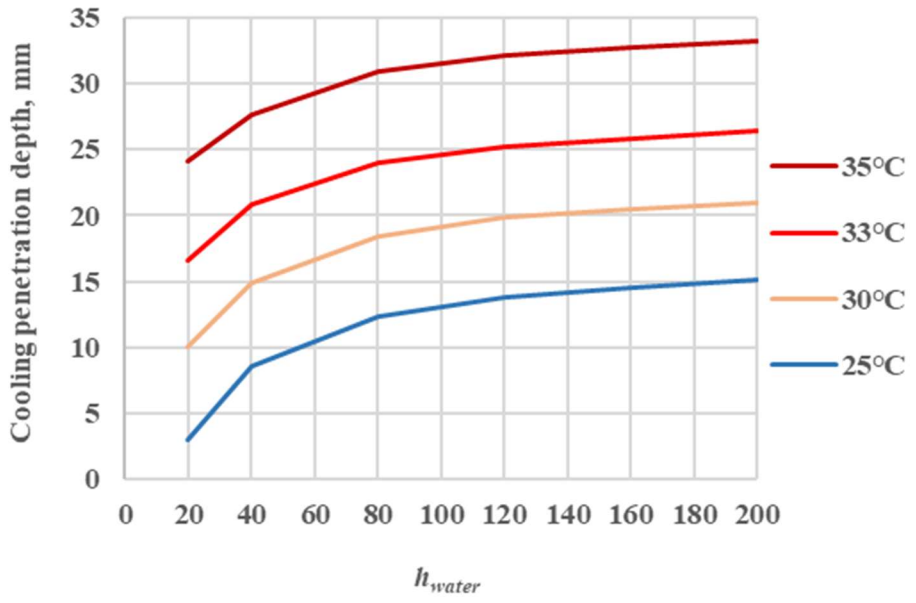

Figure 3.7: Effects of the overall heat transfer coefficient h_{water} on the cooling penetration depth after cooling of 20 minutes under a specific threshold temperature (25°C, 30°C, 33°C, or 35°C).

Chapter 4: Summary, Contribution, and Future Works

4.1 Summary

The objective of the study was to combine theoretical simulations and experimental measurements to investigate temperature fields in tissue regions near the knee of human volunteers during surface cooling. The first part of the study was to perform experiments to collect cooling pad parameters on healthy adult volunteers when applying a cooling pad to the knee. Experimental data showed that surface cooling with a coolant temperature at 0°C resulted in large temperature reductions at the skin surface after 20 minutes of cooling. The comparison of experimental results and theoretical predictions were performed to extract the unknown overall heat transfer coefficient at the skin surface (h_{water}), varying from 116 - 248 W/m^2 K. Finally, the study was to simulate temperature fields in the human tissue to assess cooling penetration targeting the tissue site during surface cooling. The results demonstrate effectiveness of reducing tissue temperatures at surface cooling. However, the cooling strongly depends on the temperature of the coolant. On the contrary, the resulted temperature field in the tissue is weakly affected by the overall heat transfer coefficient at the skin surface, especially when h_{water} is larger than 200 W/m^2 K. The maximal penetration depth of cooling after 20 minutes with a threshold temperature of 35°C is 34 mm, which is achieved with a coolant temperature at 0°C and h_{water} at 200 W/m^2 K. If the patients prefer to use 20°C tap water as coolant, the cooling penetration depth is still 26 mm from the skin surface. We believe that the theoretical simulation data could be incorporated into simple formulas for clinicians to make decision whether to prescribe cold therapy to patients after surgery, depending on the surgical site.

4.2 Contribution to the Field

Unlike experimental studies using animal models or human volunteers, quantitative 3-D thermal modeling is a powerful tool to help clinicians improve their ability to deliver safe and effective therapy. The major contribution of the current study is the development of a whole-body heat transfer model to provide detailed steady state and transient temperature distributions in tissue to evaluate the effectiveness and safety of cold therapy using a surface cooling pad. The detailed temperature fields in the deep tissue regions can be used by clinicians to evaluate whether the cooling penetration reaches the targeted surgical site based on what kind of coolant to use, thus, deciding whether to prescribe cold therapy to patients. Cold therapy may be effective if the targeted region is within 26 mm or 34 mm under the skin surface when the coolant temperature is 20°C or 0°C, respectively. In addition, the theoretical simulations can provide data on cooling penetration beyond typical cooling sessions of 20 minutes for patients if the patients can tolerate longer cooling durations. Although we did not expect significant differences in the cooling penetration in tissue when the cooling pad is placed on another body location, the whole-body model can be modified slightly to evaluate its performance on other parts of the body.

The current study has a broader impact on society via providing an alternative method to reduce pain after surgery. Future experiments are needed to evaluate correlations between local pain relief and tissue temperature reduction. If the cooling pad approach is an effective method to relieve pain, then it has the potential to decrease the number of patients turning to opioid use for immediate pain relief.

Therefore, it will add brakes to the widespread opioid epidemic of the past two decades.

4.3 Limitation and Future Works

One major limitation of this study is the small sample size of the experimental study. Despite the small sample size, we noticed large variations on the recorded temperatures and temperature decay rates among the three healthy volunteers. In the future, the experiments can be expanded to include more volunteers. This is to evaluate whether there are differences between male and female, and whether age plays a role in the temperature field. Further, experiments should be repeated for each volunteer to evaluate repeatability of the measured data. In addition, the IRB approval only allows experiments to be performed on healthy volunteers. The data would be more convincing if patients who had surgery are included in the study. This would need research collaboration with surgeons from clinics or hospitals. Such experiments including both healthy volunteers and patients after surgery would further illustrate different baseline physiological parameters and different responses to cooling.

There are several limitations on the developed whole body heat transfer model. One is due to an assumed baseline blood perfusion rate of muscle. The baseline blood perfusion rate and local metabolism may vary from one volunteer to another. The variation would affect the resulted simulation temperature of a cooling session. If the infrared images can be calibrated or improved, it can be used to extract the baseline values of blood perfusion and metabolism. However, this requires knowing of the emissivity value of the skin.

We are puzzled by the variation of the extracted values of h_{water} among the three volunteers, since in theory the value should be the same when the coolant flow rate is kept the same. It is possible, the variation of the extracted h_{water} values might be due to the inaccuracy of the baseline blood perfusion rate and metabolism. In future studies, one probably could perform a two-parameter curve fitting of the recorded temperatures on the skin surface during the cooling session to extract not only the h_{water} value, but also the baseline blood perfusion rate and metabolism. The predicted results of the theoretical model on the cooling penetration depth would be greatly improved with accurate cooling and physiological parameters.

During the experiment, the volunteers were asked to wear shorts to expose the skin surface of the lower extremities. The rest of the body was covered by clothing. It is a limitation of the study to use a uniform h_{air} value. Due to the clothing layer, the value of h_{air} of the rest of body surfaces should be much smaller than 9.57 W/m^2 K, if the clothing layer is not included in the model. The added conduction resistance of the clothing layer would decrease the overall heat transfer coefficient at these skin surfaces. Another approach to address the limitation could be adding a clothing layer in the model via keeping the same overall heat transfer coefficient h_{air} as 9.57 W/m^2 K. Other improvements in the model include accurate representation of the human geometry. In the current model, simple structures such as rectangular columns or cylinders were used to construct the model. In future study, tapering columns may be used to realistically represent the body components, especially in the cooling region such as the knee.

Although this study models the entire body, the resulted temperature field in the knee region is not significantly affected by the rest of the tissue region. In the future,

when the computational resources are limited, one would only need to include the tissue region in the vicinity of the cooling pad to have fast simulations and yet resulting in acceptable accuracy of the results.

4.4 Conclusion

A combined experimental and theoretical simulation approach was developed to evaluate the performance of a surface cooling pad in reducing temperatures in human knee tissue. Experiments were performed on healthy volunteers to collect skin temperature values under a cooling pad during a cooling session of 20 minutes. Then a whole-body heat transfer model was developed to extract the unknown overall heat transfer coefficient. Parametric studies were conducted to investigate the effects of the coolant temperature and overall heat transfer coefficient on the tissue temperature field. The simulations resulted in demonstrated the effectiveness of the cooling pad in reducing temperatures by at least 2°C (37°C to 35°C) within a tissue region less than 34 mm under the cooling pad. This was achieved with a coolant temperature of 0°C for a cooling duration of 20 minutes. We conclude that theoretical simulations based on experimental inputs are particularly useful to understand tissue temperature fields and to evaluate the effects of various cooling parameters during a cooling session. Results of this study would provide clinicians quantified information on whether to prescribe cooling therapy to patients after surgery.

References

1. Abramson, D., Rejal, H., and Fleischer, C. *Relationship Between a Range of Tissue Temperature and Local Oxygen Uptake in the Human Forearm. I. Changes Observed Under Resting Conditions.* The Journal of Clinical Investigation, 37(7):1031-1038, 1958.

2. Augustine, G. J., editor. *Voltage-Dependent Membrane Permeability*. Chapter 3 in Neuroscience, 3:47-67, Purves, D., Augustine, G. J., Fitzpatrick, D., et al., editors, Sinauer Associates, 2004.

3. Bartgis, C., LeBrun, A., Ma, R., and Zhu, L. *Determination of Time of Death in Forensic Science via a 3-D Whole Body Heat Transfer Model*. Journal of Thermal Biology, 62:109-115, 2016.

4. Bergman, T. L., Lavine, A. S., Incropera, F. P., and Dewitt, D. P. *Fundamentals of Heat and Mass Transfer.* John Wiley & Sons, 8:59-561, 2011.

5. Bouganim, N., and Anatoli, F. *History of Cryotherapy.* Dermatology Online Journal, 11(2):9, 2005.

6. Carney, N., Totten, A. M., O'Reilly, C., Ullman, J. S., et al. *Guidelines for the Management of Severe Traumatic Brain Injury.* Brain Trauma Foundation, 4:36-46, 2016.

7. CDC. *Understanding the Opioid Overdose Epidemic.* Center for Disease Control and Prevention, 1:1, 2021.

8. Charlton, M., Stanley, S. A., Whitman, Z., Wenn, V., Coats, T. J., Sims, M., and Thompson, J. P. *The Effect of Constitutive Pigmentation on the Measured Emissivity of Human Skin*. PlOS One, 15(11):e0241843, 2020.

9. Chato, J. C. *A View of the History of Heat Transfer in Bioengineering*, in Bioengineering Heat transfer Advances in Heat Transfer edited by Y. I. Cho, Advances in Heat Transfer, Academic Press, 22:1-18, 1992.

10. Cleveland Clinic Medical Professional. *Cryotherapy.* Cleveland Clinic, 1:1, 2020.

11. Dhavalikar, M., Narkeesh, A., and Gupta, N. *Effects of Skin Temperature on Nerve Conduction Velocity and Reliability of Temperature Correction Formula in Indian Females.* Journal of Exercise Science and Physiotherapy, 5(1):24-29, 2009.

12. Diao, C., Zhu, L., and Wang, H. *Cooling and Rewarming for Brain Ischemia or Injury: Theoretical Analysis*. Annals of Biomedical Engineering, 31:346-353, 2003.

13. Hall, M. J., Schwartzman, A., Zhang, J., and Liu, X. *Ambulatory Surgery Data from Hospitals and Ambulatory Surgery Centers: United States, 2010.* National Health Statics Reports, 102:4-6, 2017.

14. Hoffman, W. E., Miletich, D. J., and Albrecht, R. F. *Differential Cerebral Hypothermia.* Elsevier, 19(5):392-401, 1982.

15. Kosky, P., Balmer, R., Keat, W., and Wise, G. *Exploring Engineering: An Introduction to Engineering and Design.* Elsevier, 5:317-340, 2020.

16. Li, Y., LeBrun, A., Topoleski, L. D. T., and Zhu, L. *Evaluation of Sensitivity and Accuracy of Infrared Thermography for Melanoma Screening*. Summer Biomechanics, Bioengineering, & Biotransport Conference, National Harbor, MD, Paper number SB3C-2016-145, 2016.

17. Manuchehrabadi, N., and Zhu, L. *Gold Nanoparticle Based Laser Photothermal Therapy in Handbook of Thermal Science and Engineering*. Francis Kulacki, editor-in-chief), Section: Heat Transfer in Biology and Biological Systems. Ram Devireddy, section editor, Springer International Publication, 1:1-33, 2017.

18. Maier, C. M., Sun, G. H., Cheng, D., Yenari, M. A., Chan, P. H., and Steinberg, G. K. *Effects of Mild Hypothermia on Superoxide Anion Production, Superoxide*

Dismutase Expression, and Activity Following Transient Focal Cerebral Ischemia. Neurobiol. Dis., 11:28-42, 2002.

19. Marion, D. W., Leonov, Y., Ginsberg, M., Katz, L. M., Kochanek, P. M., et al. *Resuscitative Hypothermia*. Crit. Care Med., 24(suppl):S81-89, 1996.

20. Miller, T. E., and Mythen, M. *Successful Recovery after Major Surgery: Moving Beyond Length of Stay.* Perioperative Medicine**,** 3(4), 2014

21. National Institute on Drug Abuse. *Opioid Overdose Crisis.* National Institute of Health, 1:1, 2021.

22. Pennes, H. H. *Analysis of Tissue and Arterial Blood Temperatures in the Resting Human Forearm*. Journal of Applied Physiology, 1:93– 122, 1948.

23. Pierce-Smith, D., Turley Jr, R., and Joseph, T. N., reviewers. *Ice Pack vs. Warm Compresses for Pain.* Brigham and Women's Hospital, 1:1, 2020.

24. Sensor Scientific. *Considering Different Bead Type Thermistors.* Sensor Scientific, 1:1, 2019.

25. Singh, M., Lombardo, J., Caporale, A., and Zhu, L. *Performance of Skin Cooling Device in Cooling Penetration in Tissue – Experiments and Simulations*. Paper

#242, Summer Biomedical, Bioengineering and Biotransport Conference, Eastern Shore, Maryland, June 20th, 2022.

26. Singh, M., Turnbaugh, B., Ma, R., and Zhu, L. *Managing Cooling Penetration and Minimizing Systemic Hypothermia after Surgery Using a Cooling Pad – Whole Body Heat Transfer Simulation.* Summer Biomedical, Bioengineering and Biotransport Conference, 1:1-2, 2020.

27. Smith, K., and Zhu, L. *Theoretical evaluation of a simple cooling pad in inducing hypothermia in spinal cord following traumatic injury*. Medical and Biological Engineering & Computing, 48(2):167-175, 2010.

28. Sudheendra, D., Fraser, M., and Foley, M., Reviewers. *After Surgery: Discomforts and Complications.* UC San Diego Health, 1:1, 2021.

29. Vesnovsky, O., Grossman, L. W., Casamento, J. P., Chamani, A., Zhu, L., and Topoleski, L. *Identifying Critical Design Parameters for Improved Body Temperature Measurements: A Clinical Study Comparing Transient and Predicted Temperature Measurements*. ASME Journal of Medical Devices, 13:011005(1-15), 2019.

30. Xu L., Yenari, M. A., Steinberg, G. K., and Giffard, R. G. *Mild hypothermia reduces apoptosis of mouse neurons in vitro early in the cascade*. J. Cereb. Blood Flow Metab. 22:21-28, 2002.

31. Yenari, M. A., Onley, D., Hedehus, M., deCrespigny, A., Sun, G. H., et al. *Diffusion- and Perfusion-Weighted Magnetic Resonance Imaging of Focal Cerebral Ischemia and Cortical Spreading Depression under Conditions of Mild Hypothermia*. Brain Res. 885:208-219, 2000.

32. Zelman, D., Reviewer. *Inflammation.* WebMD, 1:1, 2020.

33. Zhu, L. *Heat Transfer Applications in Biological Systems*. Chapter 2 in Biomedical Engineering & Design Handbook, Volume 1: Bioengineering Fundamentals. pp. 2.33-2.67, Myer Kutz, editor-in-chief, McGraw-Hill, 2009.